Studies of Isomeric Yield Ratios in the Production of Sc^{44}, Mn^{52}, and Y^{87} by Photonuclear Reactions*

WILLIAM B. WALTERS† AND JOHN P. HUMMEL
Department of Chemistry and Chemical Engineering and Department of Physics, University of Illinois, Urbana, Illinois

(Received 10 June 1966)

Isomeric yield ratios for the production of the Sc^{44}, Mn^{52}, and Y^{87} isomers have been measured in photonuclear reactions. Scandium, iron, manganese, cobalt, yttrium, and niobium targets were used, and they were irradiated with bremsstrahlung of maximum energy in the 100- to 300-MeV range. The observed isomeric yield ratios show a general favoring of the isomer whose spin is closer to that of the target nucleus. In those cases in which several different bremsstrahlung energies were used, there were no significant variations in the observed isomeric yield ratios with changes in the bremsstrahlung maximum energy. The observed isomeric yield ratios are compared with theoretical isomer ratios calculated on the basis of a compound-nucleus mechanism using the statistical-model formulation of Huizenga and Vandenbosch. The observed isomeric yield ratios can be reproduced by using the same values for the level-density spin-cutoff parameter that are required to account for the isomer ratios that have been observed for particle-induced reactions producing the same isomeric pairs. The required spin-cutoff parameters are reduced by 10 and 20% from those expected for a rigid body in the cases of Sc^{44} and Y^{87}. For Mn^{52} the required value is about 50% larger than the rigid-body value. The result for Mn^{52} is unusual and may be due to shell structure effects which are not included in the statistical model that was used as a basis for the calculations.

I. INTRODUCTION

DURING the last few years the study of isomeric yield ratios has become an important approach for studying the angular momentum effects in nuclear reactions.[1–12] The results of these studies have been useful in confirming the reaction mechanisms and in leading to information about the spin dependence of the nuclear level densities in the nuclei involved. Most of the isomer ratio studies to date have involved particle-induced reactions. Except for some work on (γ,n) reactions,[1,3,12] this approach has not been exploited extensively as far as photonuclear reactions are concerned. This is especially true of photonuclear reactions that proceed at energies above the giant dipole resonance where detailed information about the reaction mechanisms and the multipole nature of the photon absorption process is generally not available. Isomer ratio measurements involving the more complex photonuclear reactions could be of value in leading to such information. In addition, because a more limited range of spin states is generally populated during the course of a photonuclear reaction, the results of isomer ratio measurements on photonuclear reactions can serve as a valuable check on the conclusions obtained about the spin dependence of the nuclear level density from the results on particle-induced reactions involving similar nuclei.

We are reporting here the results of measurements of isomeric yield ratios for several photonuclear reactions that lead to the production of the Sc^{44}, Mn^{52}, and Y^{87} isomers. Most of the reactions studied involve the emission of more than one nucleon and proceed at energies above the giant dipole resonance. The results of these measurements are compared with isomer ratios calculated on the basis of a compound-nucleus mechanism and conclusions are reached about the spin-cutoff parameter that defines the spin dependence of the nuclear level density. In all cases, isomer ratio data exist in the literature for the production of these isomers in particle-induced reactions. These data are also discussed in connection with the results from the present study.

II. EXPERIMENTAL PROCEDURE

The yield ratios for the photoproduction of the Sc^{44}, Mn^{52}, and Y^{87} isomers were determined from measurements of their radioactivities in samples that had been irradiated with bremsstrahlung from the University of Illinois 300-MeV betatron. The target materials and the bremsstrahlung energies that were used are summarized in Table I. Natural target materials were used in all cases. The amount of target material that was used was 1 g in the scandium oxide irradiations and 5 to

* This work was supported by the U. S. Office of Naval Research under Contract No. NONR 1834 (05).

† Present address: Massachusetts Institute of Technology, Cambridge, Massachusetts.

[1] J. R. Huizenga and R. Vandenbosch, Phys. Rev. **120**, 1305 (1960).
[2] R. Vandenbosch and J. R. Huizenga, Phys. Rev. **120**, 1313 (1960).
[3] J. H. Carver, G. E. Coote, and T. R. Sherwood, Nucl. Phys. **37**, 449 (1962).
[4] J. L. Need, Phys. Rev. **129**, 1302 (1963).
[5] C. T. Bishop, J. R. Huizenga, and J. P. Hummel, Phys. Rev. **135**, B401 (1964).
[6] C. Riley, K. Ueno, and B. Linder, Phys. Rev. **135**, B1340 (1964).
[7] C. T. Bishop, H. K. Vonach, and J. R. Huizenga, Nucl. Phys. **60**, 241 (1964).
[8] R. Vandenbosch, L. Haskin, and J. C. Norman, Phys. Rev. **137**, B1134 (1965).
[9] I. R. Williams and K. S. Toth, Phys. Rev. **138**, B382 (1965).
[10] N. D. Dudey and T. T. Sugihara, Phys. Rev. **139**, B896 (1965).
[11] J. Bacso, J. Csikai, B. Kardon, and D. Kiss, Nucl. Phys. **67**, 443 (1965).
[12] S. Costa, F. Ferrero, S. Ferroni, L. Pasqualini, and E. Silva, Nucl. Phys. **72**, 158 (1965).

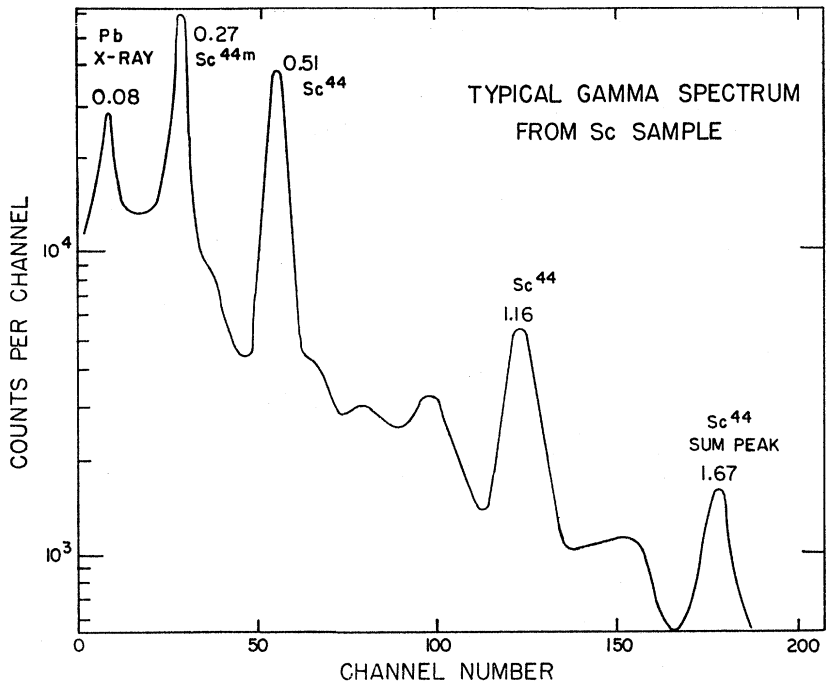

FIG. 1. Gamma-ray spectrum from a sample of scandium oxide that had been irradiated for 2 h with 223-MeV bremsstrahlung. The sample was counted for 14 h starting 73 h after the end of the irradiation. The gamma-ray energies (in MeV) and assignments are given next to each photopeak.

6 g in the other cases. Because the samples were powdered or granular in form, they were placed in Lucite holders for the irradiations. These holders were located in the collimated bremsstrahlung beam at the exit of the primary collimator. The irradiation times varied from 20 min to 10 h, depending on the half-life of the isomer being studied and the yield for the reaction of interest. Duplicate runs were made for most targets at at least one energy in order to check the reproducibility of the results. In the Sc^{44} and Y^{87} studies the yields of both the ground and metastable states could be conveniently obtained in each irradiation. In the determination of the Mn^{52} isomers, however, separate irradiations were usually used to obtain the yields of the ground and metastable states because of the large difference in their half-lives. In these experiments the bremsstrahlung beam intensities were monitored with a calibrated thick-walled copper ionization chamber that was connected to a vibrating-reed electrometer. Because equipment that was being used in other experiments was present in the beam, the monitor readings had only relative significance and no attempts were made to determine the absolute yield values for the reactions that were studied.

TABLE I. Summary of the irradiations.

Target material and purity	Isomers studied	Bremsstrahlung energies (MeV)
Scandium oxide (99.5%)[a]	Sc^{44}	50, 75, 175, 223, 264, 300
Iron metal (99.5%)[b]	Sc^{44}, Mn^{52}	100, 150, 200, 250[c]
Manganese metal (99.5%)[a]	Sc^{44}, Mn^{52}	100, 150, 225, 300[d]
Cobalt metal (99%)[a]	Mn^{52}	150
Yttrium metal (99%)[e]	Y^{87}	150, 280
Niobium metal (99.5%)[a]	Y^{87}	150, 280

[a] Supplied by Fairmount Chemical Company, Newark, New Jersey.
[b] Supplied by Merck and Company, Rahway, New Jersey.
[c] Sc^{44} studied only at 250 MeV.
[d] Sc^{44} studied only at 225 and 300 MeV.
[e] Supplied by Michigan Chemical Corporation, St. Louis, Michigan.

The radioactivity measurements were made by observing the gamma-ray spectra from the samples with a scintillation spectrometer. The irradiated samples were placed in 50-ml beakers which were placed on the top of a 3×3-in. NaI(Tl) crystal for counting.[13] The spectra were recorded by several different multichannel analyzers in which 256 or more channels were generally utilized. Each sample was counted several times in order to obtain the decay curves for the photopeaks of interest. The number of counts taken and the span of time covered varied from one sample to another, but typically ten or more counts were made on each sample over about three half-lives of the longest lived component of interest. In order to indicate the complexity of the spectra involved, some gamma-ray spectra obtained in these studies are shown in Figs. 1 to 3. These spectra are from scandium oxide, iron, and yttrium samples. The spectra observed from other target materials were of comparable complexity. However, the photopeaks of interest were easily observed in all cases.

[13] The samples were usually counted without performing any chemical separations. However, in order to observe the Mn^{52g} in the cobalt irradiations, it was necessary to chemically separate a manganese fraction. This was done by first removing cobalt by precipitating potassium cobaltinitrite and then precipitating manganese as $MnNH_4PO_4 \cdot 7H_2O$. The chemical yield of the manganese was determined from the Mn^{56} counting rates before and after the separation.

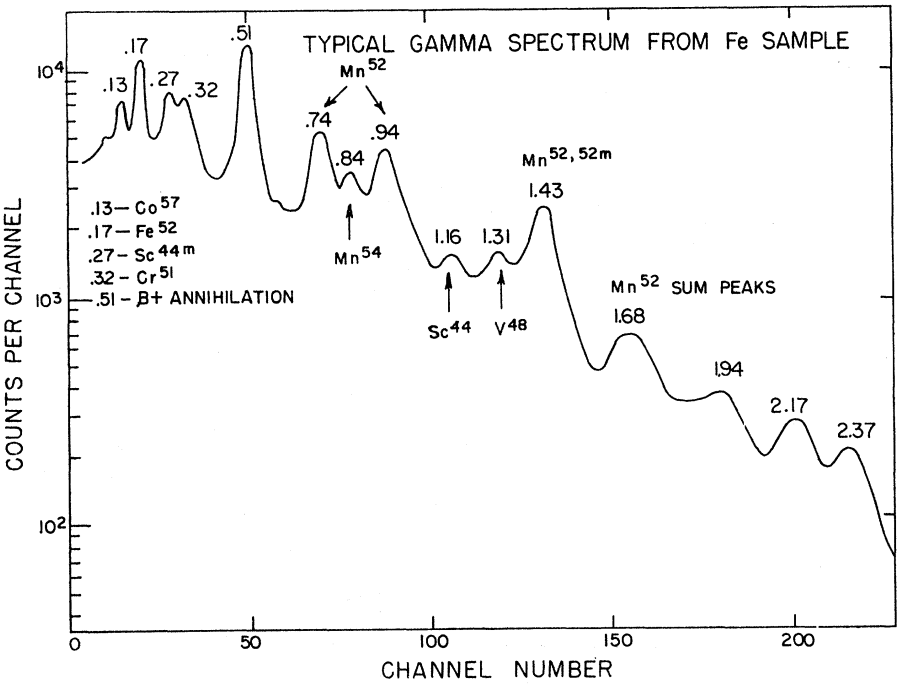

FIG. 2. Gamma-ray spectrum from an iron sample that had been irradiated for 8 h with 200-MeV bremsstrahlung. The sample was counted for 2 h starting 28 h after the end of the irradiation. The energies (in MeV) and assignments are given near each photopeak.

The decay schemes for the isomeric pairs of interest are shown in Figs. 4 to 6.[14,15] From the decay scheme for the Sc^{44} isomers shown in Fig. 4, we note that Sc^{44m} decays completely to Sc^{44g}. Thus, the growth and decay of the gamma rays associated with Sc^{44g} can be used to determine the amounts of both Sc^{44g} and Sc^{44m} that are present. We have used the 1.16-MeV gamma ray for this purpose because it is the most intense. Since only one gamma ray was used to determine the yields of both of the isomers, no counting efficiency corrections had to be applied in calculating the yield ratio.

For the determination of the Mn^{52} isomers (see Fig. 5 for a partial decay scheme showing the main transitions) the 1.43-MeV gamma ray is the most convenient radiation to use, since both Mn^{52m} and Mn^{52g} decay through the 1.43-MeV level. In this case, however, there are several complicating factors that had to be considered in determining the relative numbers of the ground- and metastable-state nuclei from the decay curve data. One involves making corrections for the different abundances of the 1.43-MeV gamma ray in the decay of the ground and metastable states and for the growth of the ground-state nuclei in the isomeric transition branch. A second factor is that the different decay schemes for the ground and metastable states give rise to different possibilities for the coincidence summing of photons in the NaI crystal. This leads to a difference of about 5% in the efficiences for observing the 1.43-MeV photopeak in the ground- and metastable-state decays. This was corrected for by calculating the probabilities for the various possible summing events using the efficiency factors given by Heath.[16] Finally, in the cases of the iron and cobalt targets, the effects of the presence of Fe^{52} as a reaction product must be considered. This decays to Mn^{52m} with an 8-h half-life and thus gives rise to an 8-h component which must be considered in the analysis of the decay curve for the 1.43-MeV gamma ray.

The decay scheme for the Y^{87} isomers is shown in Fig. 6. We have assumed that Y^{87m} decays completely by an isomeric transition to Y^{87g}, even though the absence of a significant electron capture branch has not been firmly established. (Upper limits of 15% and 0.1% for the EC/IT and β^+/IT branching ratios[17,18] have been reported.) This same assumption was used by Vandenbosch *et al.*[8] in analyzing their data on the production of the Y^{87} isomers in several charged-particle-induced reactions. From the decay scheme it appears that the best approach to use in determining the isomer ratio would be to follow the decay and growth of the 483-keV gamma ray associated with the decay of Y^{87g}. This has the disadvantage, however, that the presence of 511-keV annihilation radiation associated with positron emitters will interfere with the observation of the 483-keV photopeak. This is particularly troublesome in the case of the niobium samples. Thus, we have based our determination of the isomer ratio on the combined photopeak arising from the

[14] Unless stated otherwise, all decay scheme data including spin assignments were taken from *Nuclear Data Sheets*, compiled by K. Way *et al.* (Printing and Publishing Office, National Academy of Sciences—National Research Council, Washington 25, D. C.), NRC 60-2-16, 61-3-26, and 60-3-56.

[15] The spin assignments for the Sc^{44} isomers were taken from D. L. Harris and J. D. McCullen, Phys. Rev. **132**, 310 (1963).

[16] R. L. Heath, Atomic Energy Commission Research and Development Report No. IDO-16408, 1957 (unpublished).

[17] L. G. Mann and P. Axel, Phys. Rev. **84**, 22 (1951).

[18] E. K. Hyde and G. D. O'Kelley, Phys. Rev. **84**, 944 (1951).

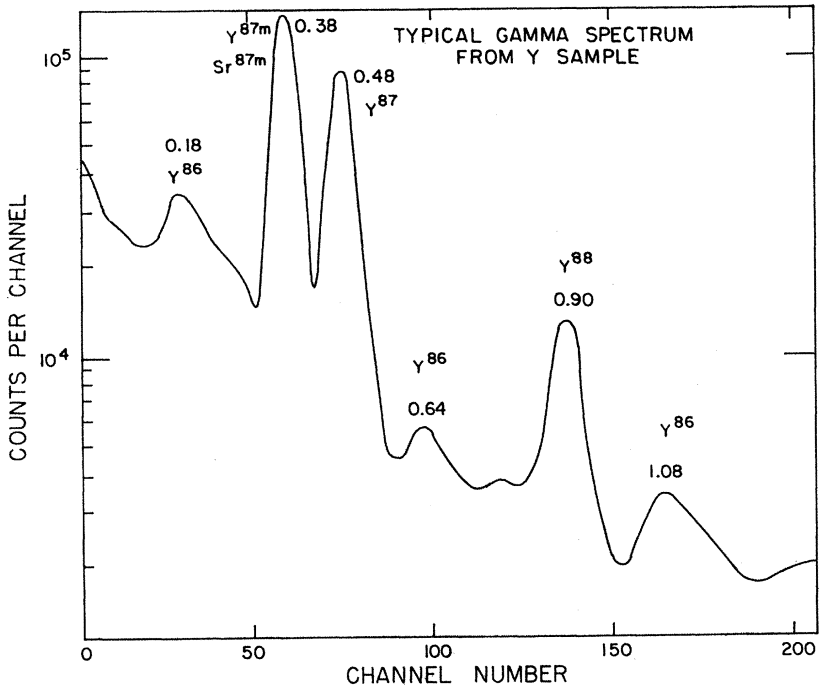

FIG. 3. Gamma-ray spectrum from a yttrium sample that had been irradiated for 8 h with 150-MeV bremsstrahlung. The sample was counted for 1.7 h starting 74 h after the end of the irradiation. The energies (in MeV) and assignments are given next to each photopeak.

381-keV isomeric transition in the decay of Y^{87m} and the 388-keV isomeric transition in the decay of Sr^{87m}. In the case of the niobium samples, the presence of Zr^{87} as a reaction product complicates the analysis of the decay curve for this photopeak because it produces Y^{87m} in its decay. Because the half-life of Zr^{87} (94 min) is relatively close to that of Sr^{87m} (2.8 h), we have encountered some difficulty in analyzing the decay curves for the 0.38-MeV photopeak to obtain accurate results for these components. This leads to relatively large uncertainties in the isomeric yield ratios for the niobium samples.

The analyses of the various decay curves obtained in this work were done by using an iterative least-squares fitting program[19] and an IBM 7094 computer. The program computed the zero-time intercepts and their standard deviations for each contributing component. These were then used in conjunction with the proper decay and growth equations to calculate the isomeric yield ratios which are reported in the next section.

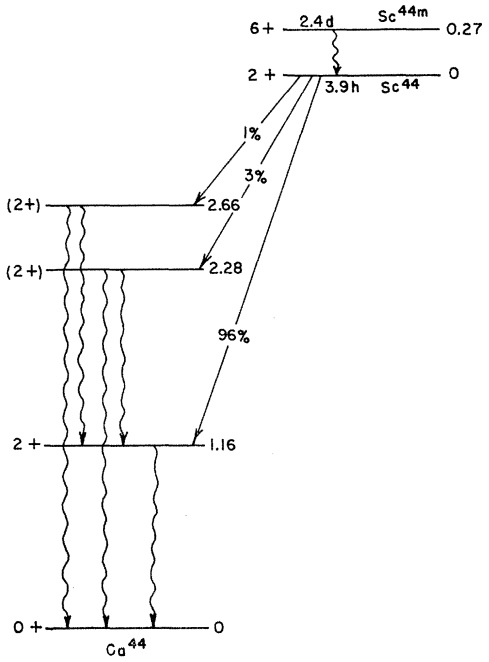

FIG. 4. Decay scheme for the Sc^{44} isomers.

TABLE II. Summary of the results for the photoproduction of the Sc^{44} isomers (spins 2 and 6).

Target isotope and spin	Bremsstrahlung energy (MeV)	Fraction of yield to high-spin isomer
Sc^{45} ($I=\frac{7}{2}$)	50	0.21±0.04
	75	0.21±0.03
	175	0.20±0.02
	223	0.18±0.01
	264	0.17±0.02
	300	0.21±0.02
$Fe^{54,56}$ ($I=0$)[a]	250	0.38±0.02
Mn^{55} ($I=\frac{5}{2}$)	225	0.42±0.04
	300	0.39±0.02

[a] It is assumed that most of the yield is due to reactions involving the two lightest isotopes present in natural iron (Fe^{54} and Fe^{56}).

[19] The least-squares fitting program was supplied to us by G. Moscati. It was based on a program described in J. L. Need and T. E. Fessler, National Aeronautics and Space Administration Report No. NASA TND-1453, 1962 (unpublished).

TABLE III. Summary of the results for the photoproduction of the Mn^{52} isomers (spins 2 and 6).

Target isotope and spin	Bremsstrahlung energy (MeV)	Fraction of yield to high-spin isomer
$Fe^{54,56}$ ($I=0$)[a]	100	0.39±0.03
	150	0.36±0.02
	200	0.35±0.02
	250	0.37±0.02
Mn^{55} ($I=\frac{5}{2}$)	100	0.44±0.04
	150	0.48±0.02
	225	0.47±0.02
	300	0.47±0.02
Co^{59} ($I=\frac{7}{2}$)	150	0.62±0.02

[a] It is assumed that most of the yield is due to reactions involving the two lightest isotopes present in natural iron (Fe^{54} and Fe^{56}).

III. EXPERIMENTAL RESULTS

The observed isomeric yield ratios for the photoproduction of the Sc^{44}, Mn^{52}, and Y^{87} isomers are summarized in Tables II to IV. The results are expressed there in terms of the fraction of the yield that populates the high-spin isomer. For Sc^{44} and Y^{87}, the high-spin isomer is the metastable state; in the Mn^{52} case, the high-spin isomer is the ground state. The uncertainties

TABLE IV. Summary of the results for the photoproduction of the Y^{87} isomers (spins $\frac{1}{2}$ and $\frac{9}{2}$).

Target isotope and spin	Bremsstrahlung energy (MeV)	Fraction of yield to high-spin isomer
Y^{89} ($I=\frac{1}{2}$)	150	0.42±0.03
	280	0.42±0.03
Nb^{93} ($I=\frac{9}{2}$)	150	0.71±0.13
	280	0.69±0.13

shown in the tables are based on the standard deviations calculated for each component by the least-squares decay-curve fitting program.

Although there are no results in the literature which can be directly compared with the results in Tables II to IV, there are results for some of the same targets for lower energy bremsstrahlung that should be compared with our results. These are summarized in Table V. A comparison of these results with those in Tables II

TABLE V. Literature data for the photoproduction of the Sc^{44} and Mn^{52} isomers.

Target element	Product nucleus	Bremsstrahlung energy (MeV)	Fraction of yield to high-spin isomer
Sc	Sc^{44}	22[a]	0.18±0.03
		24[b]	0.14±0.02
		36[b]	0.16±0.02
		48[b]	0.16±0.03
Fe	Mn^{52}	70[c]	0.32±0.05

[a] S. A. Steinberg, B. S. thesis, University of Illinois, 1963 (unpublished).
[b] Reference 38.
[c] R. M. Henry and D. S. Martin, Jr., Phys. Rev. **107**, 772 (1957).

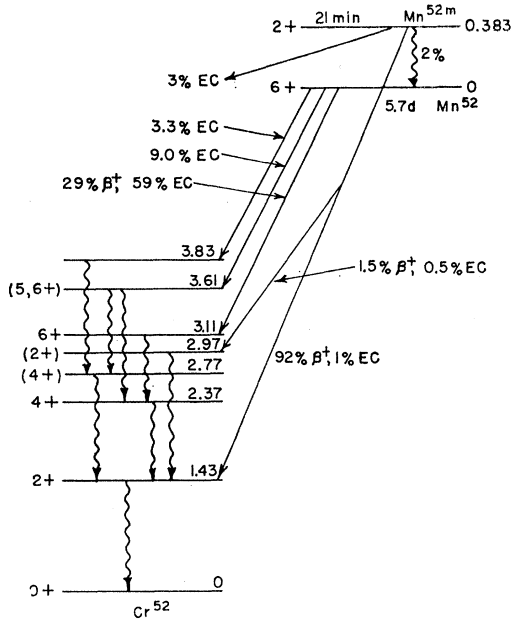

FIG. 5. Decay scheme for the Mn^{52} isomers.

and III shows that they are essentially the same as ours at the higher energies. Some additional comments on the comparison of these results to ours will be made in Sec. IV.

IV. QUALITATIVE COMMENTS ON THE RESULTS

The results given in Tables II to IV show a general favoring of the isomer whose spin is closer to that of the

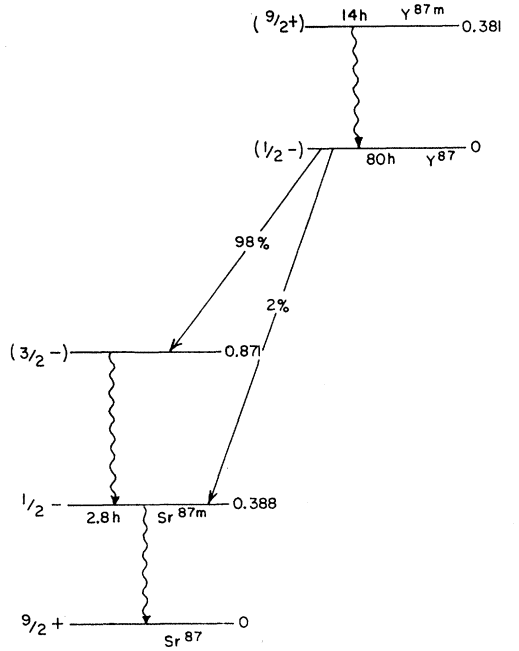

FIG. 6. Decay scheme for the Y^{87} isomers.

target nucleus. This behavior has also been observed for a large number of (γ,n) reactions[3] and is a consequence of the relatively small angular momentum changes involved in the various steps in the reactions. The results in Tables II to IV also show a tendency for the fraction of the yield to the isomer closer in spin to that of the target nucleus to decrease as the number of particles emitted in the reaction increases. Thus, as the amount of angular momentum that can be carried away by the emitted particles increases, the influence of the target spin in determining the isomer ratio is diminished.

Another feature of the results given in Tables II to IV is that in those cases in which several different bremsstrahlung energies were used the observed isomeric yield ratios do not show any significant variation with a change in the bremsstrahlung maximum energy. This trend is observed to hold to even lower energies for the Sc^{44} and Mn^{52} results given in Table V. This constancy of an isomer ratio over a wide range of bremsstrahlung energies has also been observed by Meyer[20] for the production of the Sc^{44} isomers in vanadium targets. He found that the fraction high-spin yield was constant at 0.43 ± 0.03 from 65 to 300 MeV. Studies at lower energies on (γ,n) reactions have also shown a tendency for the yield ratios to remain relatively constant with changes in the bremsstrahlung energy at least for energies well above the reaction thresholds. For example, the fraction high-spin yield for the $Br^{81}(\gamma,n)Br^{80}$ reaction is constant at 0.29 ± 0.01 from 25 to 70 MeV.[21] However, as the reaction threshold is approached, the fraction high-spin yield begins to drop considerably.[21,22]

In order to determine the reason for this independence of the yield ratios with respect to changes in the bremsstrahlung maximum energy at energies well above the reaction thresholds, it is helpful to first note the relationship between the yield of a photonuclear reaction and the reaction cross section. This is given by

$$Y(E_0) \propto \int_0^{E_0} \sigma(E_\gamma) N(E_\gamma,E_0) dE_\gamma , \qquad (1)$$

where $Y(E_0)$ is the reaction yield when the bremsstrahlung maximum energy is E_0, $\sigma(E_\gamma)$ is the reaction cross section for photons of energy E_γ, and $N(E_\gamma,E_0)$ is the number of photons of energy E_γ in the continuous bremsstrahlung spectrum. Since the shape of the bremsstrahlung spectrum[23] is approximately given by E_γ^{-1}, the cross sections at the higher energies are weighted rather lightly and could easily give rise to an insignificant contribution to the yield. Although relatively little is known in detail about the cross-section behavior of photonuclear reactions at energies above about 30 MeV, it appears that the cross sections at the higher energies (>100 MeV) for the reactions of interest to us will generally be small enough relative to those nearer threshold that they will not contribute much to the reaction yields.[20,24–26] Thus the isomeric cross-section ratios could undergo sizeable changes in the energy range we have used and still not cause the yield ratios to change very much as the bremsstrahlung energy is changed. Using some of the known cross-section data for reactions similar to those involved in our study,[20,24] we have estimated that the isomeric cross-section ratios could change by a factor of 2 or more before the resulting changes in the yield ratios would be larger than our experimental uncertainties. Thus, we feel that the constancy of the isomeric yield ratios that we observe is mainly due to the fact that most of our observed yields are due to reactions that proceed at energies well below the lowest bremsstrahlung maximum energies that we have used and does not indicate much about the behavior of the cross-section ratios at the higher energies.

V. STATISTICAL-MODEL CALCULATIONS

We shall compare the observed isomeric yield ratios for the simpler reactions that we have studied with ratios calculated on the basis of the statistical model for compound-nucleus processes. We expect that the model should be applicable to these reactions because their yields are mainly due to reactions that are proceeding at relatively low energies (less than about 50 MeV), where the validity of the compound-nucleus mechanism should be quite good. Since the features of the statistical model as it applies to the calculation of isomer ratios have been discussed in detail by Huizenga and Vandenbosch,[1,2] by Need,[4] by Vandenbosch, Haskin, and Norman,[8] and by Dudey and Sugihara,[10] we will only outline enough of the model to indicate the parameters needed in the calculations and comment on the choices of the various parameters that we have used.

In calculating the isomer ratio it is necessary to follow the angular momentum distribution throughout the various steps of the reaction. In a photonuclear reaction these steps are the initial absorption of a photon producing the excited compound nucleus, the subsequent decay of the compound system by the emission of one or more particles producing the product nucleus of interest in an excited state, and the de-excitation of the excited product nucleus by a gamma-ray cascade leading to the ground or isomeric state.

We have usually assumed that the photon absorption process is dipole in nature. Although it appears that this

[20] R. A. Meyer, Ph.D. thesis, University of Illinois, 1963 (unpublished).
[21] A. M. King and A. F. Voigt, Phys. Rev. **105**, 1310 (1957).
[22] L. Katz, L. Pease, and H. Moody, Can. J. Phys. **30**, 476 (1952).
[23] L. I. Schiff, Phys. Rev. **83**, 252 (1951).
[24] J. R. Van Hise, R. A. Meyer, and J. P. Hummel, Phys. Rev. **139**, B554 (1965).
[25] T. T. Sugihara and I. Halpern, Phys. Rev. **101**, 1768 (1956).
[26] W. C. Barber, W. D. George, and D. D. Reagan, Phys. Rev. **98**, 73 (1955).

is the situation in the 15- to 20-MeV region (giant dipole resonance),[27] there is very little experimental evidence that this is true at higher photon energies where most of the reactions that we have studied have their largest cross sections. Therefore, we have also made some calculations in which quadrupole absorption processes have been assumed in order to see how sensitive the results are to the nature of the gamma-ray absorption process. The spin distribution of the compound nucleus has been obtained by assuming that the population of each possible spin state is proportional to its statistical weight, $(2J+1)$. The justification for this has been discussed by Huizenga and Vandenbosch.[1,2]

In the particle emission steps the populations of the various possible final spin states are governed by the transmission coefficients for the various allowed orbital angular momentum values and the density of levels of each spin. The transmission coefficients that we have used were taken from Auerbach and Perey[28] for neutrons, from Feshbach *et al.*[29] for protons, and from Huizenga and Igo[30] for alpha particles. The neutron and alpha particle values are optical-model results, while those for protons are from a square-well calculation. The appropriate energy to use for selecting the transmission coefficients was taken as $2T$ (where T is the nuclear temperature) for neutron emission and the Coulomb-barrier height for charged particle emission. Vandenbosch *et al.*[8] have shown that these are reasonable approximations for the average energies of evaporated particles. Bishop[31] has shown that in isomer ratio calculations it is reasonable to use the average energy to approximate the average effect for the spectrum of energies actually emitted.

The level density as a function of angular momentum was taken as[32]

$$\rho(J)=\rho(0)(2J+1)\exp[-J(J+1)/2\sigma^2], \qquad (2)$$

where $\rho(0)$ is the density of levels for zero angular momentum and contains most of the energy dependence for the level density and σ is a parameter (spin-cutoff parameter) which characterizes the distribution. The parameter σ can be calculated from

$$\sigma^2=\mathcal{I}t/\hbar^2, \qquad (3)$$

where $\mathcal{I}$ is a moment of inertia and t is the thermodynamic temperature. We have allowed the moment of inertia to vary, using rigid-body values in some calculations and larger or smaller values in other calculations. We have used a shifted Fermi gas model to relate the temperature with the excitation energy. The necessary relationships and parameters have been recently discussed in detail by Vandenbosch *et al.*,[8] and we will not describe them here except to note that we have normally used values for the level-density parameter[33] a given by $A/8$ MeV^{-1}.

The gamma-ray cascade that ultimately leads to the ground or isomeric state of interest was assumed to involve dipole radiation until the final step. The number of gamma rays in the cascade was calculated in the manner described by Vandenbosch *et al.*[8] Since the treatment of the gamma-ray cascade is not considered to be completely satisfactory, a variation of about one in the number of gamma rays in the cascade should probably be allowed when comparing the calculated and experimental isomer ratios.

The calculations of the angular momentum distributions in the various steps of the reactions were done with an IBM 7094 computer. The computer program that we have used is similar to one that is described by Hafner *et al.*[34]

It should be noted that the basic Huizenga-Vandenbosch formalism[1,2] which we have used as a basis for making the isomer ratio calculations does not include the effects on the spin populations caused by assuming that there is a limiting or cutoff spin above which the level density is zero (in order to exclude arbitrarily high spins) or caused by competition with other modes of decay of the compound nucleus. Dudey and Sugihara[10] have investigated these effects for several charged-particle-induced reactions and have found them to be important in determining isomer ratios. Their calculations show that, for emitting states whose spin values are in the vicinity of the cutoff spin, competition effects can be extremely important in modifying the spin populations in the product nucleus. For emitting states of much lower spin, the effects seem to be unimportant. Thus, the effects will be important for those cases in which a sizeable fraction of the spin distribution is in the region of the cutoff spin. This will often be the case in charged-particle-induced reactions because of the large amounts of angular momentum that can be brought in by the projectile. In photonuclear reactions where the spin distribution will be concentrated at angular momentum values that are below the the cutoff spin, we expect that there will be little effect on the isomer ratio. In order to see if this is the case, we have made some isomer ratio calculations in which the limiting spin and competition effects have been included. This was done by arranging to set the level density in each step equal to zero above a specified J value and by correcting the spin distribution for losses to competing processes by multiplying the

[27] D. H. Wilkinson, Ann. Rev. Nucl. Sci. **9**, 1 (1959).
[28] E. H. Auerbach and F. G. J. Perey, Brookhaven National Laboratory Report No. BNL 765 T-286, 1962 (unpublished).
[29] H. Feshbach, M. Shapiro, and V. F. Weisskopf, U. S. Atomic Energy Commission Report No. NYO-3077, 1953 (unpublished).
[30] J. R. Huizenga and G. J. Igo, Argonne National Laboratory Report No. ANL-6373, 1961 (unpublished).
[31] C. T. Bishop, Argonne National Laboratory Report No. ANL-6405, 1961 (unpublished).
[32] H. A. Bethe, Rev. Mod. Phys. **9**, 84 (1937); C. Bloch, Phys. Rev. **93**, 1094 (1954).
[33] D. W. Lang, Nucl. Phys. **26**, 434 (1961).
[34] W. L. Hafner, Jr., J. R. Huizenga, and R. Vandenbosch, Argonne National Laboratory Report No. ANL-6662, 1962 (unpublished).

TABLE VI. Calculated isomer ratios based on the statistical model for the simpler photonuclear reactions.

Reaction	E_γ (MeV)	σ/σ_R	Fraction of yield to high-spin isomer
Scandium oxide target experimental result (223 MeV) = 0.18±0.01			
$Sc^{45}(\gamma,n)Sc^{44}$	18[a]	1.0	0.21–0.26
		0.9	0.15–0.21
		0.8	0.10–0.16
		1.0[b]	0.27–0.34
	20	1.0	0.20–0.25
Manganese target experimental result (100 MeV) = 0.44±0.04			
$Mn^{55}(\gamma,3n)Mn^{52}$	47[a]	1.0	0.26–0.31
		1.5	0.48–0.50
		1.0[b]	0.29–0.34
	43	1.0	0.22–0.27
	49	1.0	0.26–0.31
Iron target experimental result (100 MeV) = 0.39±0.03			
$Fe^{54}(\gamma,np)Mn^{52}$	33[a]	1.0	0.08–0.09
		1.5	0.16–0.19
		1.0[b]	0.11–0.13
	36	1.0	0.10–0.12
$Fe^{56}(\gamma,3np)Mn^{52}$	65[a]	1.0	0.22–0.27
		1.5	0.45–0.46
		1.0[b]	0.24–0.30
Yttrium target experimental result (150 MeV) = 0.42±0.03			
$Y^{89}(\gamma,2n)Y^{87}$	33[a]	1.0	0.48–0.56
		0.8	0.34–0.46
		1.0[b]	0.52–0.60
	30	1.0	0.44–0.51
	36	1.0	0.51–0.58

[a] Energy chosen for comparison with the experimental results.
[b] Quadrupole gamma ray absorbed in first step.

distribution before each emission process by a competition function that gives for each J value the fraction of those nuclei that populate the product of interest. The limiting spin values have been calculated from the formulas given by Dudey and Sugihara[10] and the competition functions have been estimated from their graphs of partial decay fractions versus J. The results of these calculations when compared with those in which these two features were not included confirm that for photonuclear reactions the results are quite insensitive to the inclusion of the limiting spin and competition features. Thus, we have not included these refinements in most of our calculations on photonuclear reactions.

A final point that should be commented on before proceeding to the results of our calculations is the way that we have chosen to compare the experimental and theoretical results. As noted in Sec. IV, the measured photonuclear reaction yield is related to an integral of the cross-section function times the bremsstrahlung spectrum [see Eq. (1)]. Thus, in order to calculate a theoretical yield ratio to compare with our experimental results, we would have to know the theoretical cross-section ratio over the range of energies involved in the bremsstrahlung spectrum. In order to reduce the number of calculations that we had to make, we chose to make the comparison of the experimental and theoretical results in a different way rather than by using a rigorously calculated theoretical yield ratio. The approach we have used is to compare the experimental yield ratio with a theoretical cross-section ratio calculated for an incident-photon energy that corresponds to the average photon energy at which the reactions are proceeding. This average energy was calculated by weighting the photon energies in the bremsstrahlung beam by the reaction cross-section function and the bremsstrahlung spectrum, i.e., by using

$$\bar{E}=\frac{\int_0^{E_0} E_\gamma \sigma(E_\gamma) N(E_\gamma,E_0) dE_\gamma}{\int_0^{E_0} \sigma(E_\gamma) N(E_\gamma,E_0) dE_\gamma}. \quad (4)$$

Because of the absence of cross-section data for the reactions that we have studied [except for the $Mn^{55}(\gamma,3n)$ reaction from threshold to 60 MeV [35]], we have had to estimate the cross-section curves for the reactions of interest by using cross-section data for other similar reactions and adjusting the energy scales for the differences in the threshold energies.[20,24,26] The validity of this approach for comparing the theoretical and experimental isomer ratios was checked by making an extensive series of calculations in which some rigorously calculated yield ratios were compared with the cross-section ratios for the average reaction energies. The results indicate that this approach is satisfactory.

VI. RESULTS OF CALCULATIONS AND DISCUSSION

The results of the calculations of the isomer ratios based on the statistical model are given in Table VI for the simpler photonuclear reactions that we have studied. The appropriate experimental results are also given there for comparison with the calculated ratios. In the case of the iron target, we expect that most of the observed yield is due to reactions involving the two lightest isotopes, Fe^{54} and Fe^{56}, so we have included calculated values for both reactions. It is difficult to estimate the relative contributions of the two reactions because of the scarcity of high-energy photonuclear reaction yield data. However, using the available yield data for reactions at these energies,[36] we estimate that the main contribution will be from Fe^{54}, with the contribution from Fe^{56} being of the order of a few percent. It should also be noted that even though we have included results for the iron reactions for only those reaction paths that involve neutron emission first, we have made calculations for other paths and the results are essentially the same.

[35] R. L. Hines, Phys. Rev. **105**, 1534 (1957).
[36] R. J. Debs, J. T. Eisinger, A. W. Fairhall, I. Halpern, and H. G. Richter, Phys. Rev. **97**, 1325 (1955). See also Refs. 20, 24, 25.

An examination of Table VI shows that several different results are quoted for each reaction. Also, for each result a range of values for the calculated isomer ratio is given. This range arises from allowing a variation of one in the number of cascade gamma rays emitted. The several different results quoted for each reaction are given to indicate the sensitivity of the results to the choices for some of the input data involved in the calculations. The first photon energy given for each reaction is the energy that corresponds to the average reaction energy [Eq. (4)] for the bremsstrahlung energy of interest. Results for other energies are also given to show the effect of an error in calculating the proper photon energy for comparison purposes because of the uncertainties in the reaction cross-section curves that were used in the $\bar{E}$ calculations. Several different values for the spin-cutoff parameter σ have been used. These are indicated in the column labeled σ/σ_R in terms of their values relative to the value calculated from Eq. (3) for a rigid-body moment of inertia.[37] Also given in Table VI are some results for cases in which the gamma-ray-absorption step was considered to be quadrupole rather than dipole in nature.

Upon comparing the experimental and calculated isomer ratios, it appears that the results for the production of Sc^{44} and Y^{87} are fit best by using spin-cutoff parameters that are reduced slightly from the rigid-body values. For Sc^{44}, a value of σ/σ_R of about 0.9 seems to work well. For Y^{87}, a value of σ/σ_R of about 0.8 is needed. For the reactions producing Mn^{52}, on the other hand, a spin-cutoff parameter that is much larger than the rigid-body value is required. A value of σ/σ_R of 1.5 works fairly well for the $Mn^{55}(\gamma,3n)$ reaction and could account for the iron data if a fairly large fraction of the yield is due to the $Fe^{56}(\gamma,3np)$ reaction. It should be noted that these conclusions are somewhat dependent on the choice of some of the parameters used in the calculations, but it is difficult to adjust the parameters enough to obtain fits with the experimental data by using rigid-body values for the spin-cutoff parameters.

Tatarczuk and Medicus[38] also compared their experimental isomer ratios for the $Sc^{45}(\gamma,n)$ reaction with calculations based on the statistical model. However, they did not allow the spin-cutoff parameter to vary with excitation energy. They concluded that a value for σ of 2.5 ± 0.25 accounted for their results. Although we allowed σ to vary with the excitation energy, the average value was about 2.2 for the $\sigma/\sigma_R=0.9$ case. Thus, the two sets of results are in quite good agreement.

As indicated previously, these isomeric pairs have also been studied by others in particle-induced reactions. Some of these results have been reported together with detailed calculations of the type outlined here, but many have not. Two cases in which detailed calculations were included are the study of the $K^{41}(\alpha,n)Sc^{44}$ reaction by Dudey and Sugihara[10] and the study of the production of Y^{87} from Y^{89} compound nuclei by Vandenbosch *et al.*[8] In both cases, competition effects were investigated. They were found to be important in the $K^{41}(\alpha,n)$ reaction case but unimportant in the Y^{87} studies. The results on the $K^{41}(\alpha,n)$ reaction at 10 MeV (which would involved a Sc^{45} compound-nucleus excitation energy comparable to that in the photonuclear case) require a spin-cutoff parameter that is 76% of the rigid-body value. Their calculations were based on a value for the level-density parameter a given by $A/10.7$ MeV^{-1} and on a constant temperature of 1.5 MeV for excitation energies below 10 MeV. We estimate that the effect on their calculations of using a value of $A/8$ MeV^{-1} for the level-density parameter and an energy-dependent temperature would be to yield a spin-cutoff parameter that is about 15% larger which would be in good agreement with our results for the $Sc^{45}(\gamma,n)Sc^{44}$ reaction. In the case of the Y^{87} studies of Vandenbosch *et al.*, they concluded that when using a shifted Fermi gas model with a level-density parameter given by $A/8$ MeV^{-1}, a spin-cutoff parameter that is 80% of the rigid-body value is needed. This agrees nicely with our results. This agreement about the spin-cutoff parameters that are required to fit the results for the photonuclear and particle-induced reactions leading to Sc^{44} and Y^{87} indicates that the use of the compound-nucleus mechanism to describe these photonuclear reactions is valid.

Since there are no detailed calculations on the isomer ratios expected for particle-induced reactions leading to Mn^{52}, we have done the necessary calculations for energies that correspond to the compound-nucleus excitation energies encountered in our work. This requires that the spin distribution following the absorption of the incoming projectile be known. This was calculated from[2]

$$P(J_c)\propto\sum_{S=|I-s|}^{I+s}\sum_{l=|J_c-S|}^{J_c+S}\frac{2J_c+1}{(2s+1)(2I+1)}T_l(E), \quad (5)$$

where I is the spin of the target nucleus, s is the intrinsic spin of the incoming projectile, J_c is the angular momentum of the compound nucleus, and $T_l(E)$ is the transmission coefficient for the incoming projectile with orbital angular momentum l and energy E. The isomer ratios resulting from these calculations for several reactions leading to the production of Mn^{52} are given in Table VII along with the appropriate experimental results.[39,40] In doing these calculations we have used the Huizenga-Vandenbosch formalism which does not include the effects of a limiting spin or of

[37] The rigid-body moment of inertia was calculated from $\mathcal{I}_R=2MAR^2/5$, where M is a nucleon mass and R is the nuclear radius. A radius parameter r_0 of 1.2×10^{-13} cm was used.

[38] J. R. Tatarczuk and H. A. Medicus, Phys. Rev. **143**, 818 (1966).

[39] J. Wing, J. R. Huizenga, and M. Zirin, unpublished data quoted in J. Wing, Argonne National Laboratory Report No. ANL-6598, 1962 (unpublished).

[40] J. Wing and J. R. Huizenga, Phys. Rev. **128**, 280 (1962).

TABLE VII. Isomer ratios for the production of Mn^{52} in particle-induced reactions.

Reaction	E_{proj} (MeV)	σ/σ_R	Fraction of population to high-spin isomer Calculated	Experimental
$V^{50}(\alpha,2n)Mn^{52}$	22	1.0	0.78–0.83	0.83±0.03[a]
		1.5	0.89–0.90	
$V^{51}(\alpha,3n)Mn^{52}$	38	1.0	0.81–0.85	0.87±0.03[a]
		1.5	0.91–0.93	
$Cr^{52}(p,n)Mn^{52}$	10	1.0	0.10–0.12	0.20±0.02[b]
		1.5	0.19–0.21	

[a] Reference 39. [b] Reference 40.

competition with other reactions. We note that the results for the $Cr^{52}(p,n)Mn^{52}$ reaction are consistent with a much larger spin-cutoff parameter than the rigid-body value. The results for the $V^{50}(\alpha,2n)$ and the $V^{51}(\alpha,3n)$ reactions, on the other hand, seem to be more consistent with a smaller value. If the effects of a limiting spin and competition are included, however, these will tend to make some of the high-spin states unavailable for the production of Mn^{52} and will reduce the fraction high-spin yield. The effect will be large for the alpha-particle-induced reactions because a large fraction of the initial spin distribution will involve high-spin nuclei but will be relatively small for the $Cr^{52}(p,n)$ case because of the lower initial spins involved. The effect of this would be to require a larger value of the spin-cutoff parameter to fit the observed isomer ratios for the $V^{50}(\alpha,2n)$ and $V^{51}(\alpha,3n)$ reactions than before and would tend to make all of the results for both photonuclear and particle-induced reactions consistent with each other, i.e., all reactions would now be accounted for by using a spin-cutoff parameter that is much larger than the rigid-body value.

At this point we might note that the production of the Sc^{44}, Mn^{52}, and Y^{87} isomers in the more complicated photonuclear reactions that we studied can also be accounted for by statistical-model calculations using the same spin-cutoff parameters that were required for the simpler reactions. Thus, a compound-nucleus mechanism can account for the more complicated reactions. We also note here that we have calculated the isomer ratios for several different reaction paths (sequences of particles emitted) for these reactions. The results are insensitive to the paths chosen which indicates that isomer ratio measurements cannot be used to obtain detailed information about the reaction paths for compound-nucleus processes.

The observation of spin-cutoff parameters that are slightly reduced below the rigid-body values for the Sc^{44} and Y^{87} cases is similar to the behavior seen in many other nuclei for which isomer ratio measurements have been made.[3,8,41] This reduction is usually thought to be due to pairing interactions which favor the coupling of nucleons to zero angular momentum. However, attempts to quantitatively account for the reductions of the spin-cutoff parameters in terms of an independent pairing model or in terms of a superconductor model have not been completely satisfactory.[8,41] Thus, these reductions do not appear to be completely understood as yet.

The observation of the much larger than rigid-body spin-cutoff parameter in the case of Mn^{52} is an unusual result. It should be noted that a similar situation has been observed for reactions leading to the production of the Br^{80} and the Mo^{91} isomers in that spin-cutoff parameters about 50% larger than the rigid-body values are required.[3,41] There is a possibility that shell structure effects may be responsible for this behavior. Newton[42] has included shell effects in his treatment of the nuclear level density by introducing the average degeneracies of the neutron and proton states in the vicinity of the Fermi level. In medium-mass nuclei, the effect of using Newton's approach is to mainly cause reductions in the spin-cutoff parameters near the closed shells by 10 to 20%.[3] An increase in the spin-cutoff parameter by 50% cannot be accounted for by Newton's approach. It thus appears that if shell effects are responsible for the large increases in the spin-cutoff parameter, some other approach that involves a more detailed consideration of the shell structure of the individual nuclei is needed.

ACKNOWLEDGMENTS

We wish to acknowledge the work of the engineering and operating staff of the University of Illinois Betatron Laboratory in making the irradiations possible. We would also like to acknowledge the help of Dr. R. A. Meyer during preliminary experiments, Dr. F. L. Brooks in programming the isomer ratio calculation, and J. Drake in analyzing data and helping with the calculations. We would also like to thank Dr. G. Moscati for supplying us with his least-squares decay-curve analysis program. The computer calculations were done at the University of Illinois Digital Computer Laboratory which was supported by a grant from the National Science Foundation. One of us (W. B. W.) held a National Science Foundation predoctoral fellowship during part of the time that this work was in progress.

[41] H. K. Vonach, R. Vandenbosch, and J. R. Huizenga, Nucl. Phys. **60**, 70 (1964).
[42] T. D. Newton, Can. J. Phys. 34, 804 (1956).